Electronic Supplementary Material (ESI) for Chemical Communications.

Supporting Information

Synthesis and properties of poly(1,3-dioxolane) in-situ quasi-solid-state electrolytes via rare-earth triflate catalyst

Guanming Yang,[a] Yanfang Zhai,[a] Jianyao Yao,[a] Shufeng Song,*[a] Liyang Lin,[b] Weiping Tang,[c] Zhaoyin Wen,[d] Ning Hu*[e] and Li Lu[f]

Experiment

Materials. $Sc(OTf)_3$ (98%, Aladdin) was stored in the glove box ($H_2O < 0.1$ ppm, $O_2 <$ 0.1 ppm) and used without further purification. DOL (99.8%, anhydrous, containing ~75 ppm butylated hydroxytoluene as an inhibitor, Aladdin) was chemically dried with lithium foil before used. LiTFSI (99%, Aladdin) was dried under vacuum at 60 °C for 48 h before transferred to the glove box. All the chemicals were stored in the glove box.

Synthesis of PDOL Quasi-Solid-State Electrolytes. LiTFSI was dissolved into DOL first to obtain DOL-LiTFSI solution, followed 1 mM $Sc(OTf)_3$ was dissolved into DOL with vigorous stirring to obtain concentrated DOL-$Sc(OTf)_3$ solution, subsequently appropriate amounts of the concentrated DOL-$Sc(OTf)_3$ solution was added into the DOL-LiTFSI solution with vigorous stirring to generate the PDOL quasi-solid-state electrolytes with a fixed LiTFSI concentration of 2 M and varying proportions of $Sc(OTf)_3$. DOL liquid electrolyte was also prepared as a controlled sample by dissolving 2 M LiTFSI into DOL.

Material Characterizations. DOL liquid electrolyte and PDOL quasi-solid-state electrolytes were dissolved in dimethyl sulfoxide-d_6 for measuring ^{1}H NMR and ^{13}C NMR spectroscopy. Fourier-transform infrared spectroscopy (FTIR) of the electrolytes was tested using a Thermo Scientific spectrometer in reflection mode. Raman spectra of the electrolytes were tested using a LabRAM HR Evolution spectrometer. The morphologies of the lithium metal anodes were studied by a field emission scanning electron microscope (SEM, TM4000Plus II). X-ray diffraction (XRD, PANalytical X'Pert Powder) was collected to study the crystallographic structure of electrolytes.

SEM and energy dispersive spectroscopy (EDS) were used to study the microtopography of the PDOL electrolytes and the distribution of elements in electrolytes. Differential scanning calorimetry (DSC) and thermogravimetric (TG) analyses (NETZSCH TG209F3 Tarsus) were conducted to study the thermal properties of the electrolytes in N_2 atmosphere at a heating rate of 10 °C min^{-1} from 20 °C to 80 °C and 800 °C, respectively.

The electrolytes were prepared in a transparent glass bottle, and two copper foils were embed, and their ionic conductivities were measured by electrochemical impedance spectroscopy (Autolab, 302N) from 1 MHz to 0.1 Hz. The conductivity was calculated according to the relationship: $\sigma=L/(RS)$, where L, S and R are the distance between copper foils, effective area of copper foil below the electrolyte surface, and resistance, respectively. The electrochemical stability window of the electrolytes was determined via linear sweep voltammetry (LSV) with stainless steel and lithium metal as electrodes, performed from 2 V to 7 V at scan rate of 1.0 mV s^{-1}.

Electrochemical Characterizations. Quasi-solid-state cells were assembled in 2016 coin cells using the PDOL quasi-solid-state electrolytes, $LiFePO_4$ cathode and lithium metal anode. The cathode was obtained by mixing $LiFePO_4$, super P and polyvinylidene fluoride at a weight ratio of 8 : 1 : 1 in an N-methylpyrrolildone and coated on stainless steel meshes. The $LiFePO_4$ loading was about 5 mg cm^{-2}. The glass fibre separators were used in the assembly of cells to avoid short circuit. The galvanostatic charge/discharge measurements of Li||$LiFePO_4$ cells were conducted using LAND testing system (LANHE CT2001A). The Coulombic efficiencies (CEs) of Li metal

anodes were measured in Li||Cu coin cells with Celgard 3501 separators. All the electrochemical properties were measured under room temperature (approx. 25 ^{o}C).

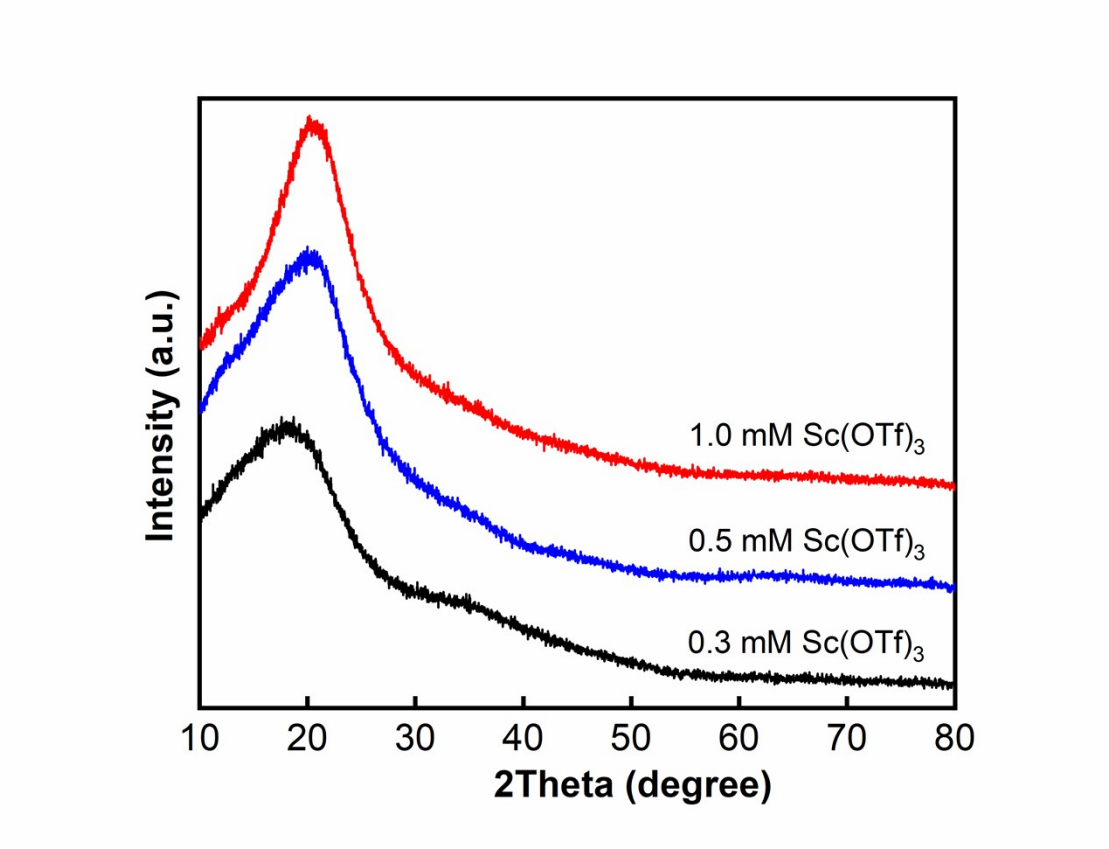

Figure S1. XRD patterns of PDOL quasi-solid-state electrolytes at 0.3, 0.5 and 1.0 mM $Sc(OTf)_3$. The XRD characterization without diffraction peak of crystallographic PDOL at about 22° illustrates the amorphous structure of the PDOL electrolytes in-situ formed in the presence of 0.3-1.0 mM $Sc(OTf)_3$

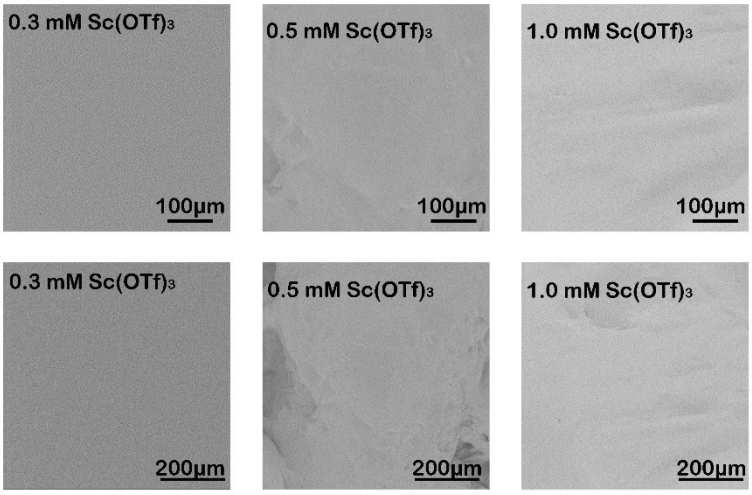

Figure S2. SEM images of PDOL quasi-solid-state electrolytes at 0.3, 0.5 and 1.0 mM $Sc(OTf)_3$.

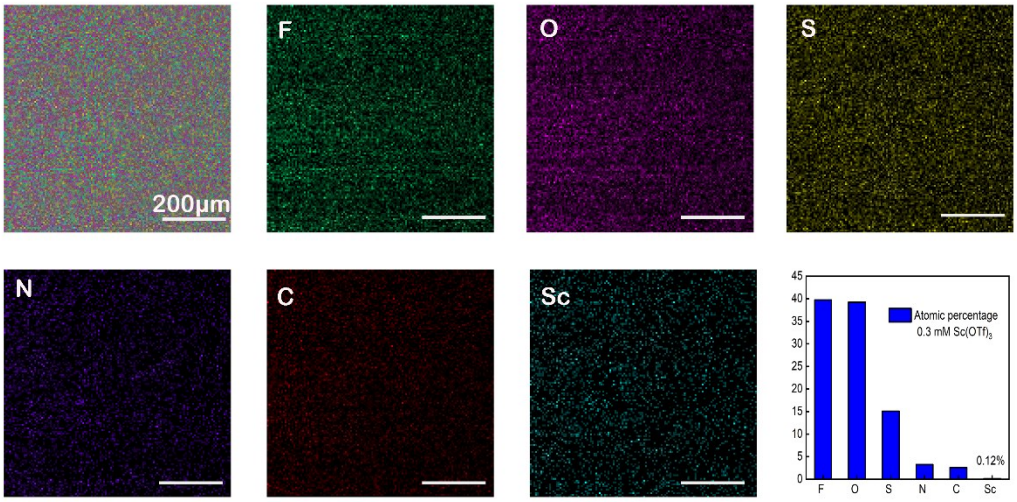

Figure S3. EDS mapping for PDOL quasi-solid-state electrolyte at 0.3 mM $Sc(OTf)_3$.

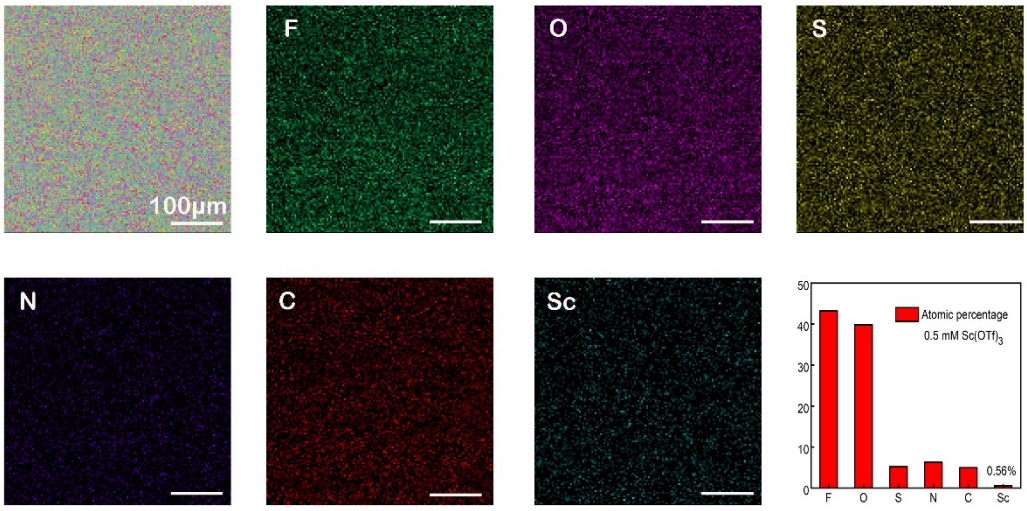

Figure S4. EDS mapping for PDOL quasi-solid-state electrolyte at 0.5 mM $Sc(OTf)_3$.

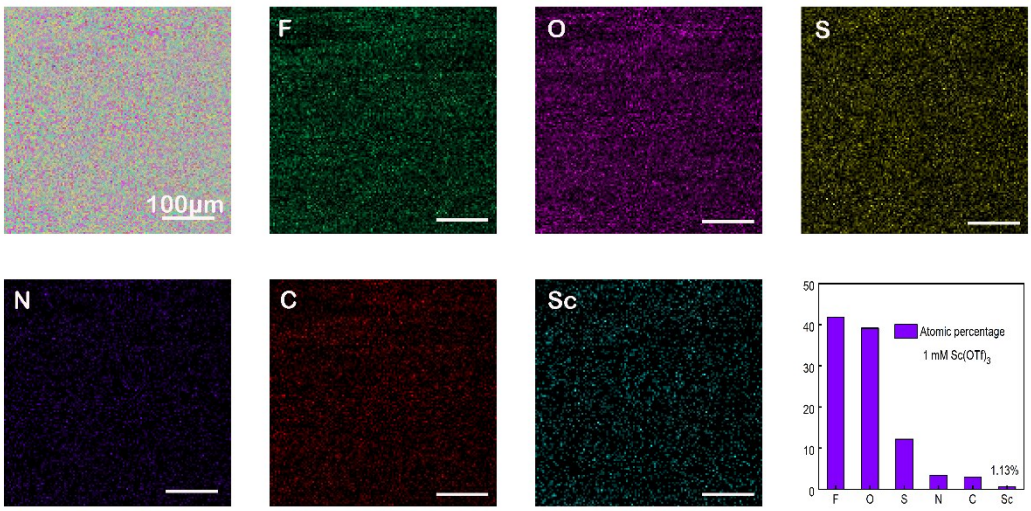

Figure S5. EDS mapping for PDOL quasi-solid-state electrolyte at1.0 mM $Sc(OTf)_3$.

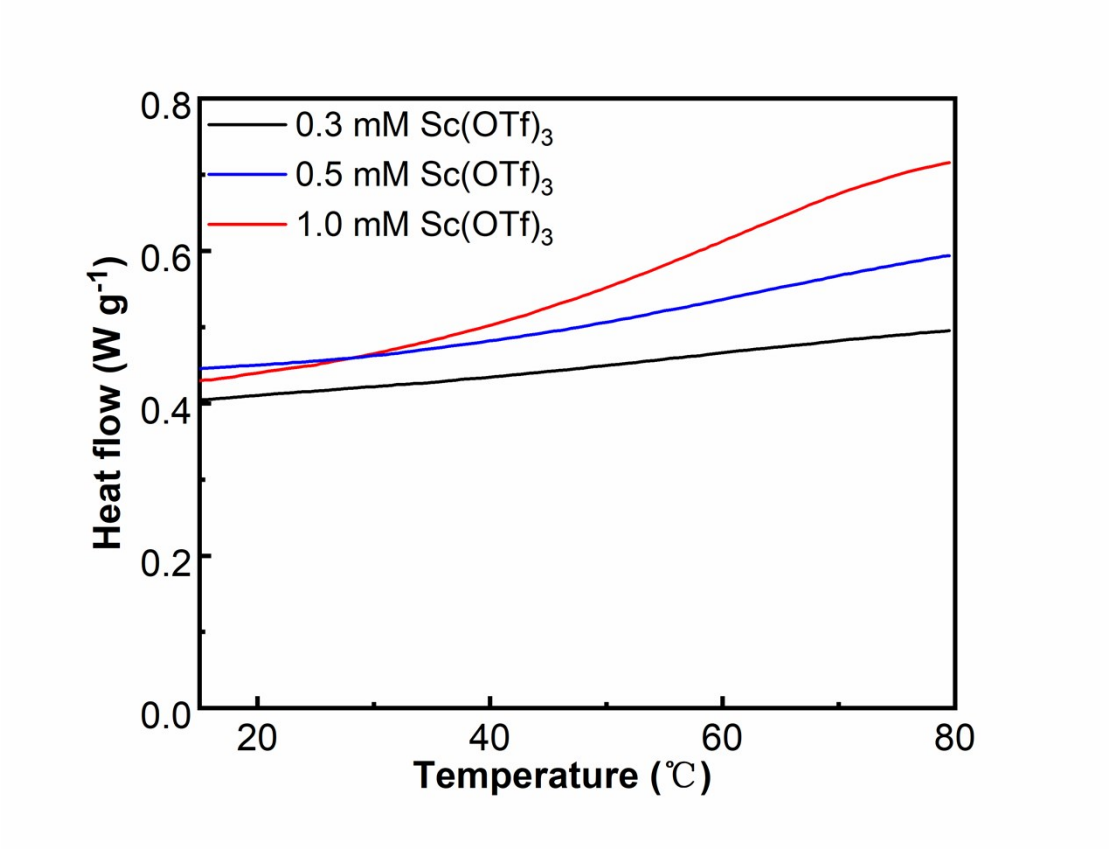

Figure S6. DSC curves of PDOL quasi-solid-state electrolytes at 0.3, 0.5 and 1.0 mM $Sc(OTf)_3$.

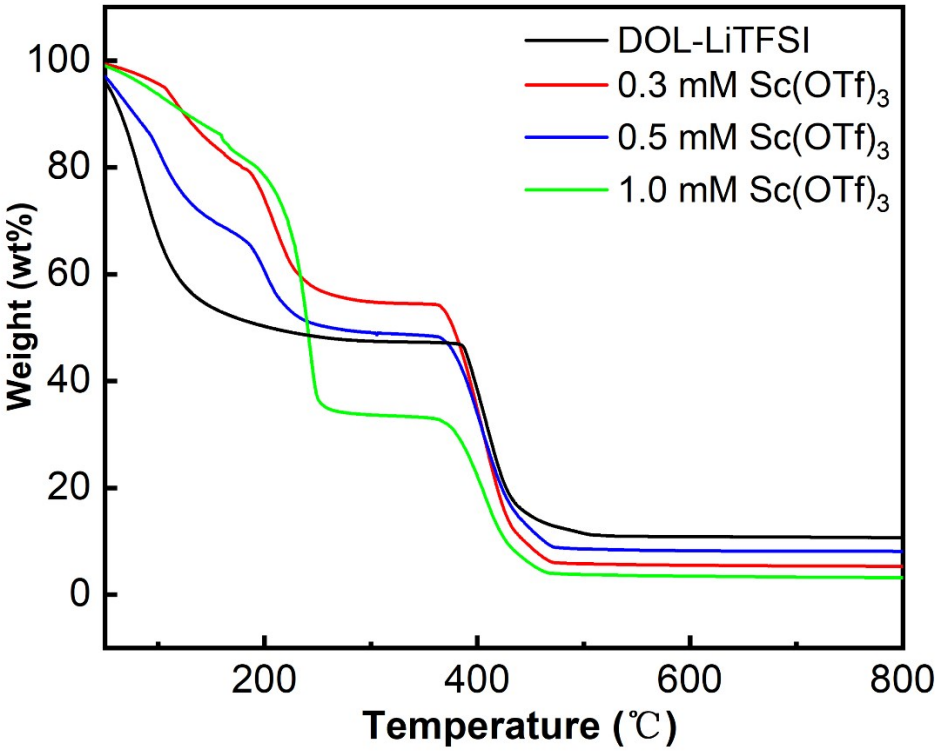

Figure S7. TG curves of DOL liquid electrolyte and PDOL quasi-solid-state electrolytes at 0.3, 0.5 and 1.0 mM $Sc(OTf)_3$.

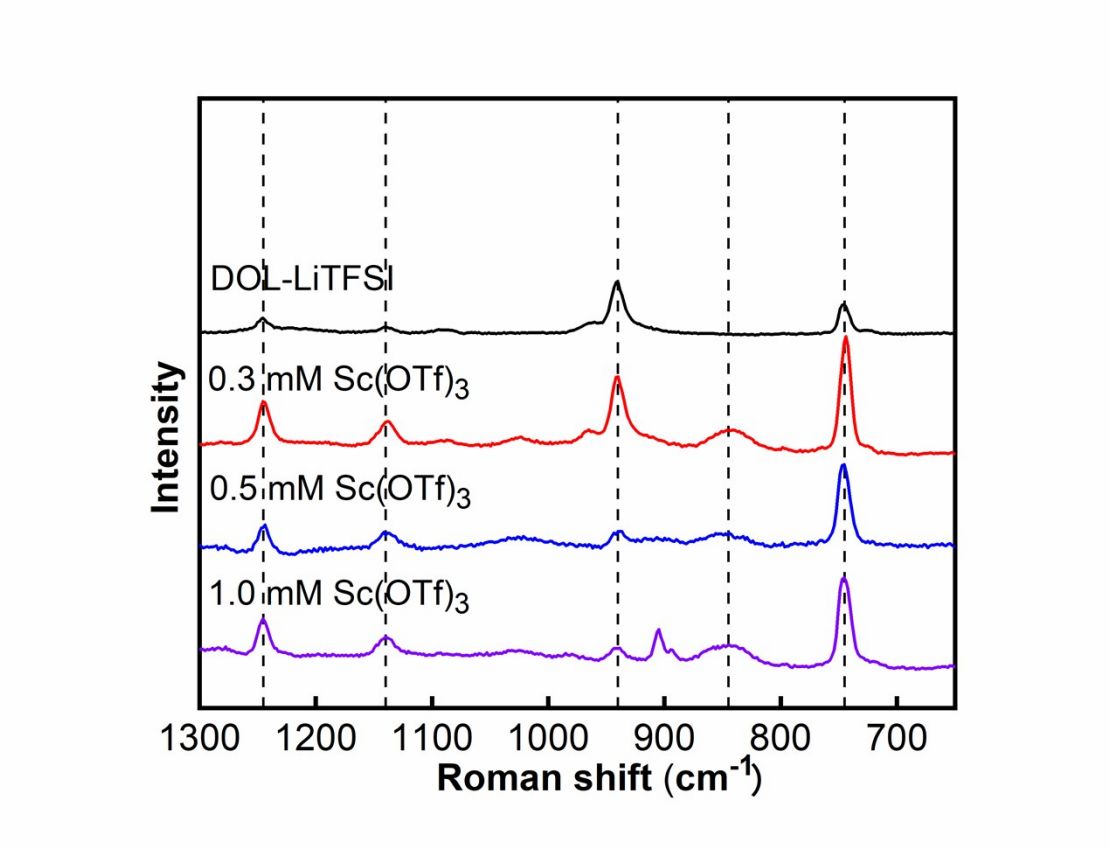

Figure S8. Raman spectroscopy of DOL liquid electrolyte and PDOL quasi-solid-state electrolytes at 0.3, 0.5 and 1.0 mM $Sc(OTf)_3$. The typical signals peaks at 1245, 1140 and 745 cm^{-1} representing the C-F stretching, C-F symmetric bending, and S-N and C-F stretching coupled with SO_2 wagging vibrations in the $TFSI^-$ anion, respectively, can be observed for all the electrolytes.[1] Upon adding $Sc(OTf)_3$, the ring stretching vibrations at 940 cm^{-1} for DOL are disappeared.[2] In the meantime, the C-H rocking and C-O stretching vibrations at 845 cm^{-1} for linear poly(1,3-dioxolane) are appeared.[3] This indicates the polymerization of DOL and is consistent with the NMR and FTIR analyses.

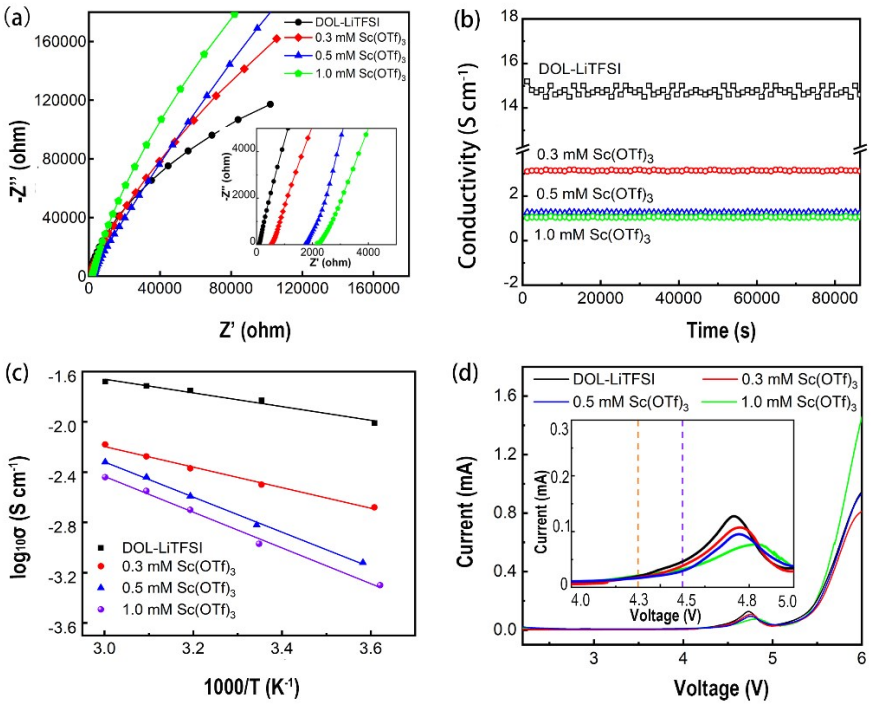

Figure S9. Electrochemical characteristics of DOL liquid electrolyte and PDOL quasi-solid electrolytes at 0.3, 0.5 and 1.0 mM $Sc(OTf)_3$. (a) Nyquist curves. (b) Conductivity versus polymerization time. (c) Conductivity versus temperature. (d) Electrochemical stability windows. The electrochemical impedance spectra of the PDOL electrolytes shown in Figure S9a only display inclined lines; this is a weak capacitance phenomenon caused by the short dielectric relaxation time, implying fast ions conduction in the PDOL electrolytes. The ionic conductivities of the PDOL electrolytes are thereby determined by the *X*-intercept to be 3.12, 1.1 and 1.07 mS cm^{-1} at 25 °C for the PDOL electrolytes formed at 0.3, 0.5 and 1.0 mM $Sc(OTf)_3$, respectively. Noting that the ionic conductivities of the PDOL electrolytes are reduced with the concentrations of $Sc(OTf)_3$ because of the abundant polymerization. The ionic conductivities remain at a relatively stable value, indicating that the polymerization reaction is very weak after 3 days proceeding though the polymerization reaction cannot approach completion.

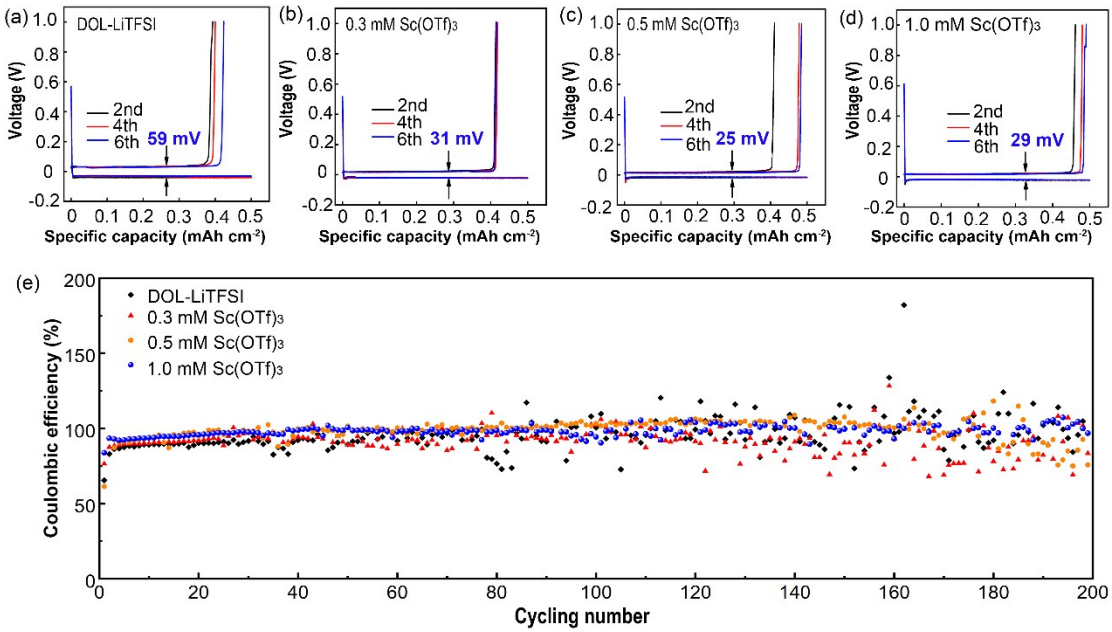

Figure S10. (a-d) Voltage profiles for the Li||Cu cells using DOL liquid electrolyte and PDOL quasi-solid-state electrolytes. Current density is 0.5 mA cm^{-2} and plating Li capacity is 0.5 mAh cm^{-2} per cycle. (e) Coulombic efficiencies as a function of cycling number for the DOL liquid electrolyte and PDOL quasi-solid-state electrolytes.

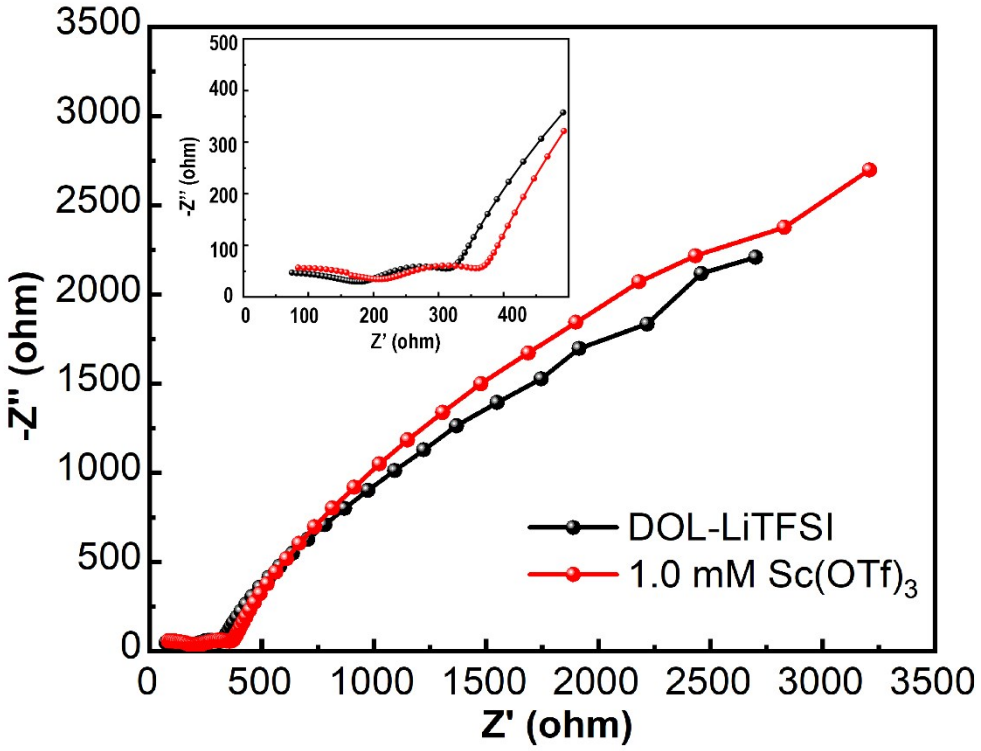

Figure S11. Electrochemical impedance spectra of Li||Cu cells using DOL liquid electrolyte and PDOL quasi-solid-state electrolyte at 1.0 mM $Sc(OTf)_3$. The Li||Cu cells using DOL liquid electrolyte and PDOL quasi-solid-state electrolyte show interfacial resistances of approx. 318 Ω and 325 Ω, respectively.

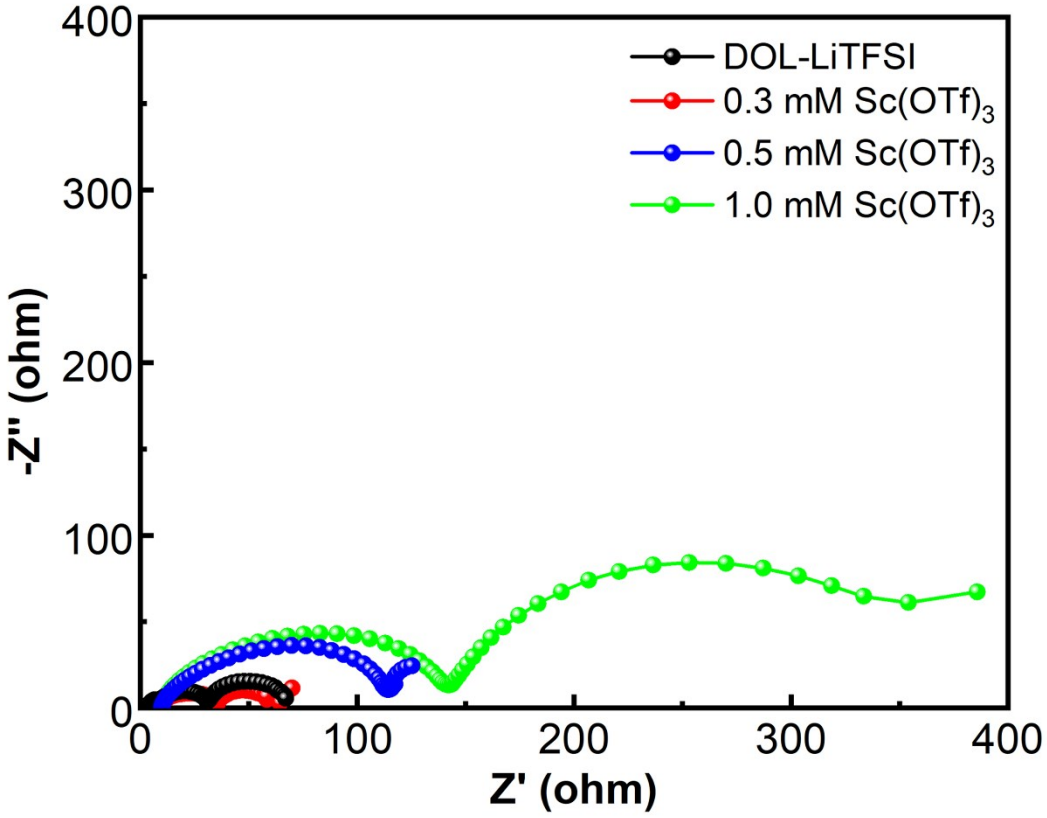

Figure S12. Electrochemical impedance spectra of Li||$LiFePO_4$ cells based on DOL liquid electrolyte and PDOL quasi-solid-state electrolytes at 0.3, 0.5 and 1.0 mM $Sc(OTf)_3$ after galvanostatic cycling.

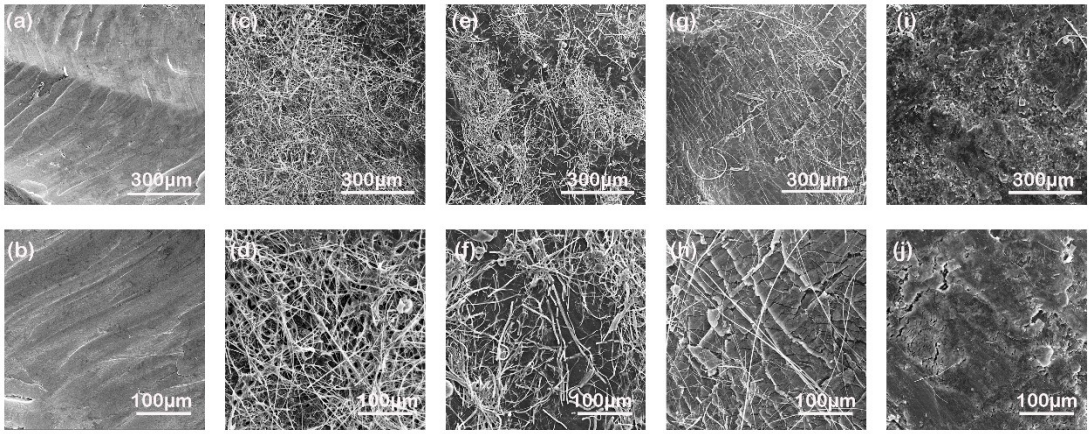

Figure S13. SEM images of cycled Li-metal anodes obtained from Li||$LiFePO_4$ quasi-solid-state cells. (a,b) pristine Li metal. (c,d) DOL liquid electrolyte. (e,f) PDOL quasi-solid-state electrolyte at 0.3 mM $Sc(OTf)_3$. (g,h) PDOL quasi-solid-state electrolyte at 0.5 mM $Sc(OTf)_3$. (i,j) PDOL quasi-solid-state electrolyte at 1.0 mM $Sc(OTf)_3$. To acquire further significative signal, scanning electron microscopy (SEM) is employed to study the morphologies of Li metal anodes after Li||$LiFePO_4$ cells cycling. As seen, the pristine Li metal displays a dense and smooth surface before cell assembly (Figure S13a,b) which has turned to fibrous Li with random orientations and length range of several hundreds of micrometer after cycling in Li/DOL/$LiFePO_4$ liquid cell (Figure S13c,d). These high-surface-area dendrites accelerate the adverse reaction of electrolyte, deteriorate the cycling stability, and lead to safety issues. In comparison, the fibrous Li dendrites are markedly eliminated for Li metal anodes in Li/PDOL/$LiFePO_4$ quasi-solid-state cells specifically at 1.0 mM $Sc(OTf)_3$ (Figure S13e-j), although a few microcracks appear, possibly because the coarse Li grains with limited interfaces influences the Li^+ consumption and thus the uniformity of the stripping process.

Reference

1 S. Suriyakumar, M. Kathiresan and A. Stephan, *ACS Omega*, 2019, **4**, 3894.

2 Q. Zhao, X. Liu, S. Stalin, K. Khan and L. Archer, *Nat. Energy*, 2019, **4,** 365.

3 D. Aurbach, O. Youngman and P. Dan, *Electrochim. Acta*, 1990, **35**, 639.